# SHALE GAS FORMATIONS IN POLAND – NEW EVALUATION METHODS FOR PROCESSING AND QUANTITATIVE INTERPRETATION USING COMPUTED X-RAY TOMOGRAPHY

*Krakowska P., *Puskarczyk E., **Jędrychowski M., ***Madejski P., *Habrat M.
*AGH University of Science and Technology in Krakow (Poland), Faculty of Geology, Geophysics and Environmental Protection
**AGH University of Science and Technology in Krakow (Poland), Faculty of Physics and Applied Computer Science
***EDF Polska SA, Research and Development in Krakow (Poland)

*This paper was prepared for presentation at the International Symposium of the Society of Core Analysts held in Vienna, Austria, 27 August – 1 September 2017*

## ABSTRACT

Computed X-ray tomography (CT) is a non-invasive method of rock analysis and provides many parameter results of shale gas formations. Samples from Silurian shale gas deposits from different regions of Poland were presented in a comparative study. Qualitative and quantitative analysis of pyrite and pore space was carried out using 2D slices and 3D models from nanotomography results as a new evaluation method. Petrophysical and mineralogical laboratory measurement results were also compared to the results obtained from CT. Evaluation of pyrite content and pore space heterogeneity offers insights about possible reservoir and geomechanical properties of shale gas deposits in Poland.

## INTRODUCTION

Unconventional oil and gas deposits in Poland are spread along a belt from the north-west to the south-east edge of Poland [1]. Hydrocarbons are accumulated in the Silurian and Ordovician formations [2, 3]. Knowledge of physical and chemical parameters of shale gas deposits brings us closer to effective hydrocarbons exploration. Moreover, proper estimation of parameters may explain why hydraulic fracturing is not conducted in a controlled manner in shale gas deposits in Poland. Heterogeneity of pore space and mineral distribution in shales plays an important role. Detailed characterization of shale heterogeneity suggests the best propositions for exploration. Pyrite, as a heavy mineral, significantly influences the mechanical properties of the rock [4]. Pores and pore channels shape also affect the reservoir and mechanical properties. Hence, the techniques of 2D and 3D rock visualization should be taken into account in sophisticated analysis.

Computed X-ray tomography (CT) is a non-invasive method of rock analysis [5, 6] and provides many parameter results of shale gas formations [7, 8]. Exemplary samples from Silurian shale gas deposits from different regions (north-west and south-east Poland) were presented and also the objects of the comparison. Qualitative and quantitative analysis of pyrite and pore space was carried out using 2D slices and 3D models from nanotomography results as a new evaluation method. Furthermore, petrophysical and mineralogical laboratory measurement results were also compared to the results obtained from CT.

## DATA SET AND METHOD

Data set comprised of samples of Silurian shale gas deposits. Samples 5, 6 and 22 were taken from a well located on the Lublin Synclinorium, south-east Poland, while sample 872 represents the shale from a well situated in the Peribaltic Syneclise, in the north-west Poland. Sample 5, 6 and 22 are from 2385.4, 2385.8, 2500.5 m depth, respectively, while 872 – from 3546 m.

The main laboratory technique, used in the analysis presented in this paper, was the computed X-ray nanotomography. Nanotom S 180n General Electric Sensing & Inspection Technologies at the Faculty of Physics and Computer Sciences, AGH UST in Krakow (Poland), is equipped with a 57-W X-ray tube. The maximum work voltage of the tube is 180 kV. Images are recorded by the Hamamatsu 2300×2300 pixel 2D detector (Ham C 7942CA-02). The maximum spatial resolution is about 500 nm. The reconstruction of measured objects was carried out using the Feldkamp algorithm for the cone beam X-ray CT. All the data was subjected to a filtering process using a 3D median filter.

Mineral composition was derived by XRD method (Table 1). Total porosity and density was estimated using a helium pycnometer. The effective porosity of 872 sample was determined by mercury porosimetry. For the samples 5, 6 and 22, Tight Rock Analysis (TRA) was conducted in Terra Tek Schlumberger Reservoir Laboratory [9, 10]. Permeability of all samples was measured using a pressure decay permeability method (Terra Tek). TRA pressure decay permeability testing was carried out on crushed shale samples at “as received” conditions. A crushed 12/20 mesh sample was weighed out to 30g and then exposed to helium gas in the reference cell. The rate at which the helium gas diffuses into the particles was monitored. No net overburden stress was applied on the sample.

P- and S-wave velocity, measured in the Laboratory of Petrophysics at Faculty of Geology, Geophysics and Environmental Protection AGH UST in Krakow (Poland), was investigated to obtain information about elastic properties.

## RESULTS

The results of XRD analysis contributed the information about the mineral composition (Table 1). In comparison to the sample 872, increase in clay mineral content is significant

in samples 5, 6 and 22, from 17% for 872 to 46% in sample 22. These results are also reflected in quartz content. Sample 22 included more pyrite than sample 872. The conclusion from these exemplary samples is as follows: geomechanical properties of shale gas reservoirs improve to the north Poland. Total porosity obtained from helium pycnometer and CT results differ because of the different measurement resolution (Table 2). Sample 22 has better reservoir parameters (e.g., higher porosity, permeability) than sample 872.

Pyrite is quite a common mineral in shale deposits. Pyrite can mainly be found in the shapes of framboids or euhedral crystals [11]. The orientation of pyrite in shale influences significantly the mechanical properties of the rock, e.g. causing uncontrolled hydraulic fracturing. The CT measurement results offered insight into the amount and orientation of pyrite in the shale samples. Pyrite content derived from the CT results is close to these obtained from XRD analysis (Table 1). Estimation of pyrite content is a new evaluation method based on CT measurement results.

2D slices from CT measurements are presented in Figure 1-4. The most bright elements represent pyrite, the most dark – pores. Figures 1-3 show 2D slices of samples 5, 6 and 22, respectively, while Figure 4 – sample 872. Samples 5, 6 and 22 differ in pyrite and pores orientation from sample 872. Pyrite predominates in the thin laminae in samples 5, 6 and 22, as opposed to the dispersed form in sample 872. In sample 5 (Figure 1) it is clear that the pyrite is developed in the form of elongated forms, while in sample 872 more spherical.

3D visualizations for samples 5, 6, 22 and 872 are presented in Figures 5-8. A transparent colour of pyrite indicates forms with volume less than 8 $\mu m^3$, red – more than 10000 $\mu m^3$. Pyrite in forms larger than 10000 $\mu m^3$ occurs sporadically. The P and S-wave velocities also indicate the weak elastic properties in samples from Lublin Synclinorium. Figure 8 shows the distribution of pyrite diameters from CT results (Table 2). The most detected pyrites have a diameter in the range of 10-20 μm in the all samples (Figure 11). Also, the diameters below 10 μm are common.

Pore space is shown in Figure 9 and 10. Pore space of sample 5 is similar to the samples 6 and 22. Sample 872 has very low porosity in the CT results – only 0.2%. Additionally, the microcrack is visible in sample 6 (green object in Figure 9). Most probably, the microcrack was naturally formed as a result of stress regime in the formation connected with the pyrite laminae appearance (e.g. lack of continuity). Moreover, microcracks are also visible in Figure 12, which resulted in increase the quantity of objects with pore diameters above 200 μm. Generally, microcracks cause increase in porosity and pore space heterogeneity.

Pore space is developed in some laminae. That is why pores are visible only in one direction and in consolidated volume (not in whole 3D visualization). The greatest amount of pores have diameters less than 10 μm (Figure 12). From the analysis of pore space distribution, samples from the Lublin Synclinorium indicate better reservoir properties. The increase in

porosity and heterogeneity of pore space distribution reduces the geomechanical properties (e.g. decrease in compressive strength, Young modulus, increase in Poissons ratio).

## CONCLUSIONS

Computed X-ray tomography is a powerful tool in petrophysical analysis of rocks. Several samples from unconventional oil and gas deposits from Poland were investigated using CT results. The conclusions are as follows:

- A new evaluation method of pyrite content estimation was presented.
- Pyrite content derived from CT results was comparable to these from XRD results.
- Pyrite occurrence and orientation in shale samples differ depending on well location.
- Pyrite in laminae was detected in samples from the south-east Poland, while in dispersed form in the whole sample from north-west Poland.
- Better reservoir parameters were identified in shale samples from south-east Poland.
- The most pyrite diameters were in the range of 10-20 μm, pores – less than 10 μm (range of micro and nanopores).

This paper presents the preliminary results of the project. The goal of the project is to analyse CT results of the tight, low porosity and low permeability shales, sandstones, limestones and dolomites, and to create and develop the software to process and interpret the CT result for the geological and petrophysical purposes (poROSE – Porous Materials Examination Software). Furtermore, project task is to analyse fluid flow in Polish tight rock.

## ACKNOWLEDGEMENTS

This project was financed by the National Centre for Research and Development in Poland, programme LIDER, project no. LIDER/319/L–6/14/NCBR/2015: Innovative method of unconventional oil and gas reservoirs interpretation using computed X-ray tomography. Computed X-ray tomography was conducted in the Laboratory of Micro and Nano Tomography in the Faculty of Physics and Applied Computer Science at the AGH University of Science and Technology in Krakow, Poland. The authors wish to thank the Polish Oil & Gas Company and Orlen Upstream for the data and core samples.

## REFERENCES

1. Porębski, S.J., Prugar, W., Zacharski, J., “Silurian shales of the East European Platform in Poland: some exploration problems”, *Geological Review*, (2013) **61**, 8, 468-477.
2. Kotarba, M .J., “Geology, ecology and petroleum of the lower Paleozoic strata in the Polish part of the Baltic region”, *Geological Quarterly*, (2012) **54**, 2, 103-108.

3. Poprawa P., "Shale gas potential of the Lower Palaeozoic complex in the Baltic and Lublin-Podlasie basins (Poland)", *Geological Review*, (2010) **58**, 3, 226-249.
4. Zhang, Ch., Dong, D., Wang, Y., Guan, Q., "Brittleness evaluation of the Upper Ordovician Wufeng–Lower Silurian Longmaxi shale in Southern Sichuan Basin, China", *Energy Exporation & Exploitation* Special Issue: Chinese Petroleum, (2017) **0(0)**, 1-14.
5. Jarzyna, J., Krakowska, P., Puskarczyk E., Wawrzyniak-Guz, K., Bielecki, J., Tkocz, K., Tarasiuk, J., Wroński, S., Dohnalik, M., "X-ray computed microtomography – a useful tool for petrophysical properties determination", *Computational Geosciences*, (2016) **20**, 5, 1155-1167.
6. Krakowska, P., Dohnalik, M., Jarzyna, J., Wawrzyniak-Guz, K., "Computed X-ray microtomography as the useful tool in petrophysics: a case study of tight carbonates Modryn formation from Poland", *Journal of Natural Gas Science and Engineering*, (2016) **31**, 67-75.
7. Josh, M., Esteban, L., Delle Piane, C., Sarout, J., Dewhurst, D.N., Clennell, M.B., "Laboratory characterization of shale properties", *Journal of Petroleum Science and Engineering*, (2012) **88-89**, 107-124.
8. Tang, X., Jiang, Z., Jiang, S. and Li, Z., "Heterogeneous nanoporosity of the Silurian Longmaxi Formation shale gas reservoir in the Sichuan Basin using the QEMSCAN, FIB-SEM, and nano-CT methods", *Marine and Petroleum Geology*, (2016) **78**, 99-109.
9. Handwerger, D., Suarez-Rivera, R., Vaughn, K., Keller, J., "Improved Petrophysical Core Measurements on Tight Shale Reservoirs Using Retort and Crushed Samples", SPE Annual Technical Conference and Exhibition, 30 October-2 November, Denver, Colorado, USA, (2011) SPE 147456, 1-19.
10. Suarez-Rivera, R., Chertov, M., Willberg, D., Green, S., Keller, J., "Understanding Permeability Measurements in Tight Shales Promotes Enhanced Determination of Reservoir Quality", SPE Canadian Unconventional Resources Conference, 30 October-1 November, Calgary, Alberta, Canada, (2012) SPE 162816, 1-13.
11. Cárdenesa, V., Merinerob, R., De Boevera, W., Rubio-Ordóñezc, A., Dewanckelea, J., Cnuddea, J.P., Booned, M., Van Hoorebeked, L., Cnuddea, V., "Characterization of micropyrite populations in low-grade metamorphic slate: A study using high-resolution X-ray tomography", *Palaeogeography, Palaeoclimatology, Palaeoecology*, (2016) **441**, 4, 924-935.

Table 1. Selected mineral content from XRD and CT results. Symbols: P CT – pyrite from CT results, P XRD – pyrite from XRD results, Q – quartz, F – feldspars, C – calcite, D – dolomite, Sc – sum of clay minerals

| Sample | P CT [%] | P XRD [%] | Q [%] | F [%] | C [%] | D [%] | Sc [%] |
|---|---|---|---|---|---|---|---|
| 5 | 1.2 | - | - | - | - | - | - |
| 6 | 1.8 | - | - | - | - | - | - |
| 22 | 2.1 | 2 | 24 | 11 | 14 | 3 | 46 |
| 872 | 0.3 | <1 | 46 | 21 | 10 | 3 | 17 |

Table 2. Petrophysical parameters. Symbols: BD – bulk density, GD – grain density, Φeff – effective porosity, Φtot – total porosity from pycnometer, Φtot – total porosity from CT results, K – absolute permeability, Vp – P-wave velocity, Vs – S-wave velocity

| Sample | BD [g/cc] | GD [g/cc] | Φeff [%] | Φtot [%] | Φtot CT [%] | K [nD] | Vp [m/s] | Vs [m/s] |
|---|---|---|---|---|---|---|---|---|
| 22 | 2.668 | 2.729 | 3.20 | 4.16 | 2.4 | 198 | 4061 | 1658 |
| 872 | 2.623 | 2.709 | 0.77 | 3.15 | 0.2 | 47 | 5054 | 2751 |

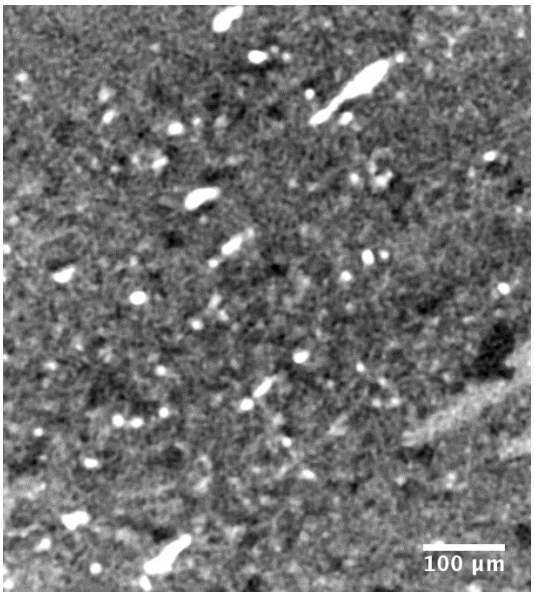


Figure 1. 2D slice of shale sample no. 5. White elements – pyrite, black – pores

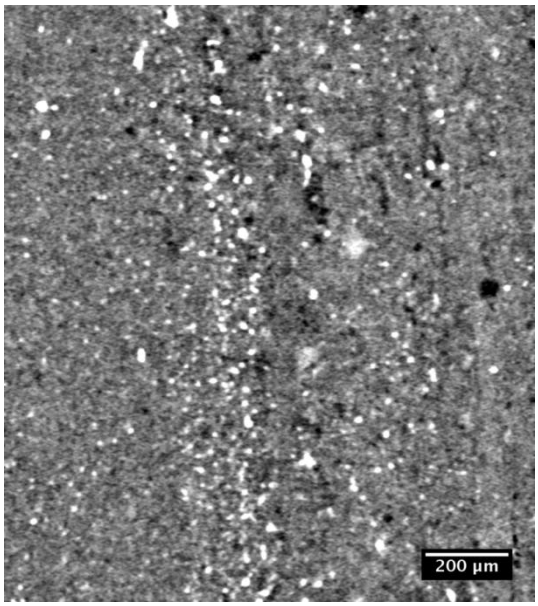


Figure 2. 2D slice of shale sample no. 6. White elements – pyrite, black – pores

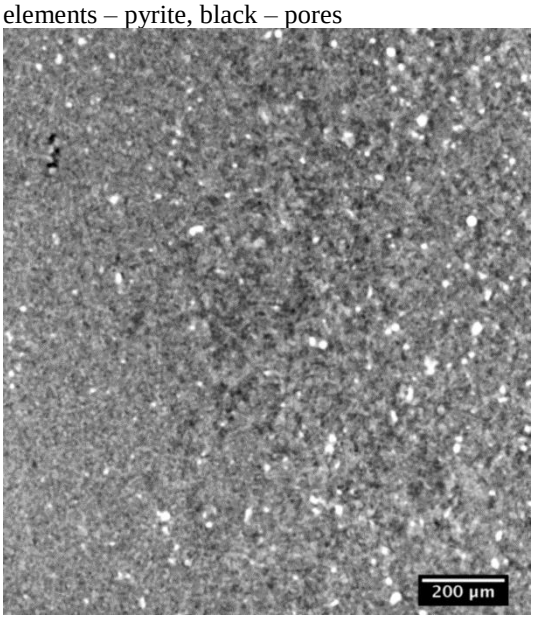


Figure 3. 2D slice of shale sample no. 22. White elements – pyrite, black – pores

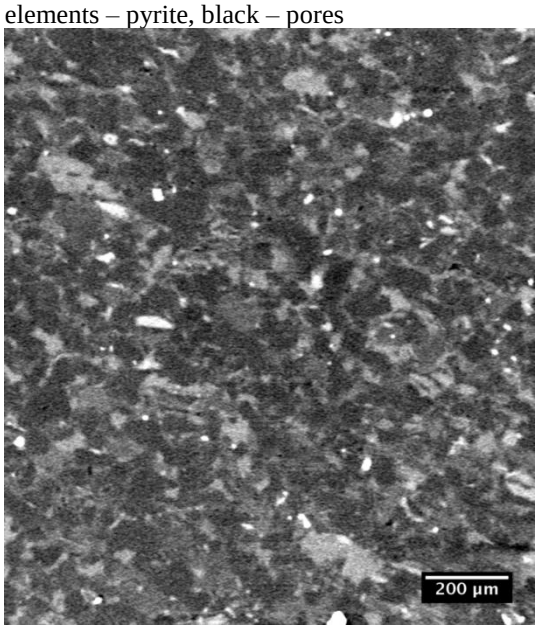


Figure 4. 2D slice of shale sample no. 872. White elements – pyrite, black – pores

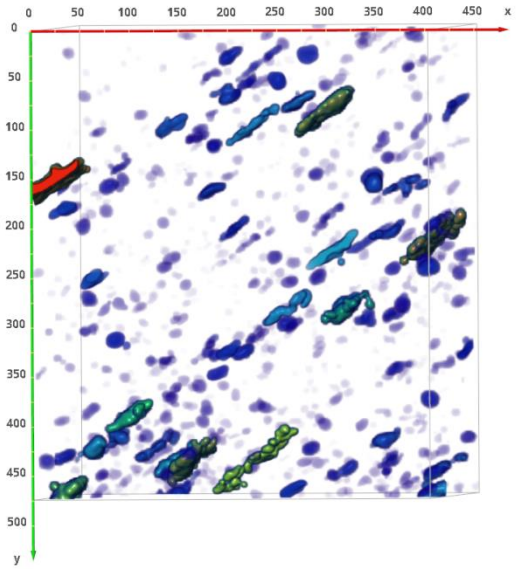


Figure 5. 3D visualization of pyrite in shale sample no. 5. Colour: transparent – less than 8 µm$^3$, red – more than 10000 µm$^3$

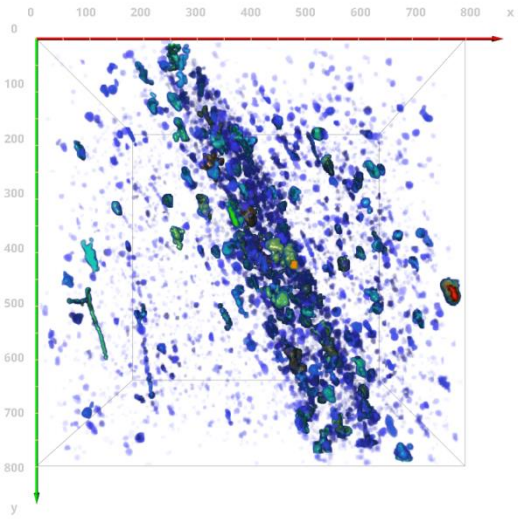


Figure 6. 3D visualization of pyrite in shale sample no. 6. Colour: transparent – less than 8 µm$^3$, red – more than 10000 µm$^3$

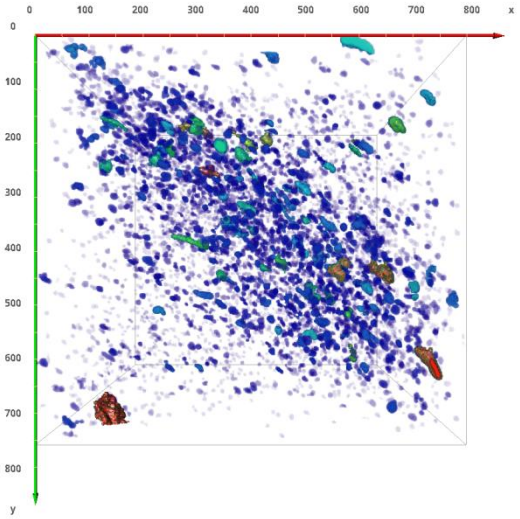


Figure 7. 3D visualization of pyrite in shale sample no. 22. Colour: transparent – less than 8 µm$^3$, red – more than 10000 µm$^3$

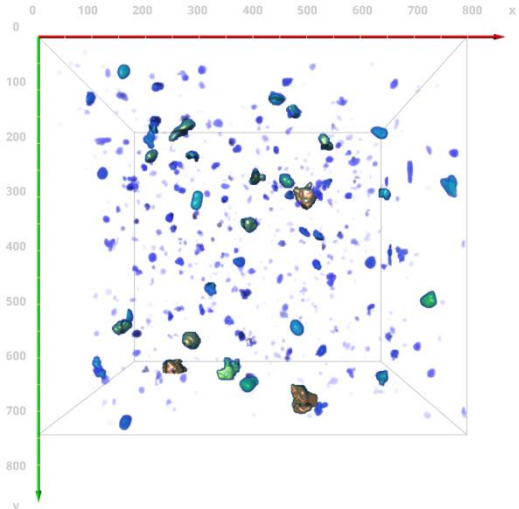


Figure 8. 3D visualization of pyrite in shale sample no. 872. Colour: transparent – less than 8 µm$^3$, red – more than 10000 µm$^3$

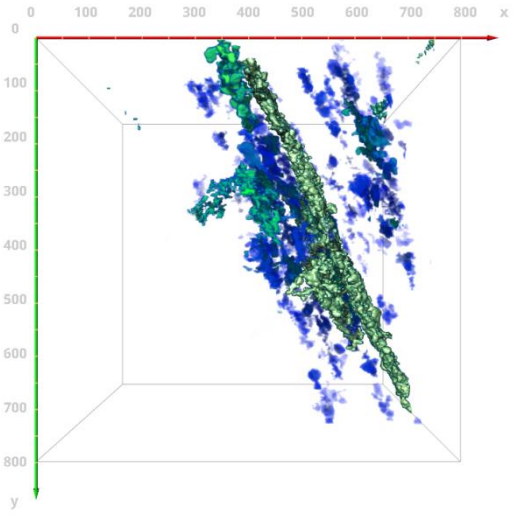


Figure 9. 3D visualization of pore space in shale sample no. 6. Colour: transparent – less than 8 µm$^3$, red – more than 800000 µm$^3$

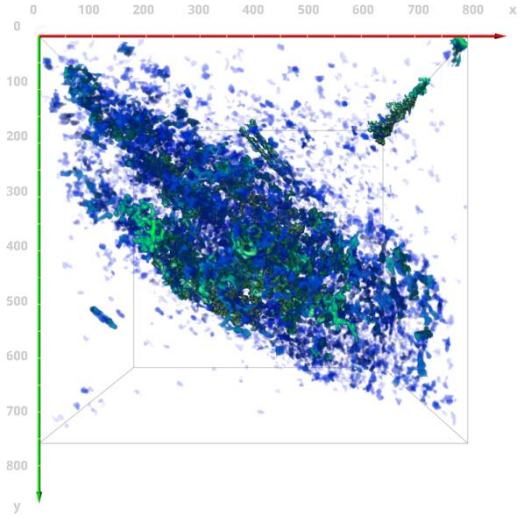


Figure 10. 3D visualization of pore space in shale sample no. 22. Colour: transparent – less than 8 µm$^3$, red – more than 100000 µm$^3$

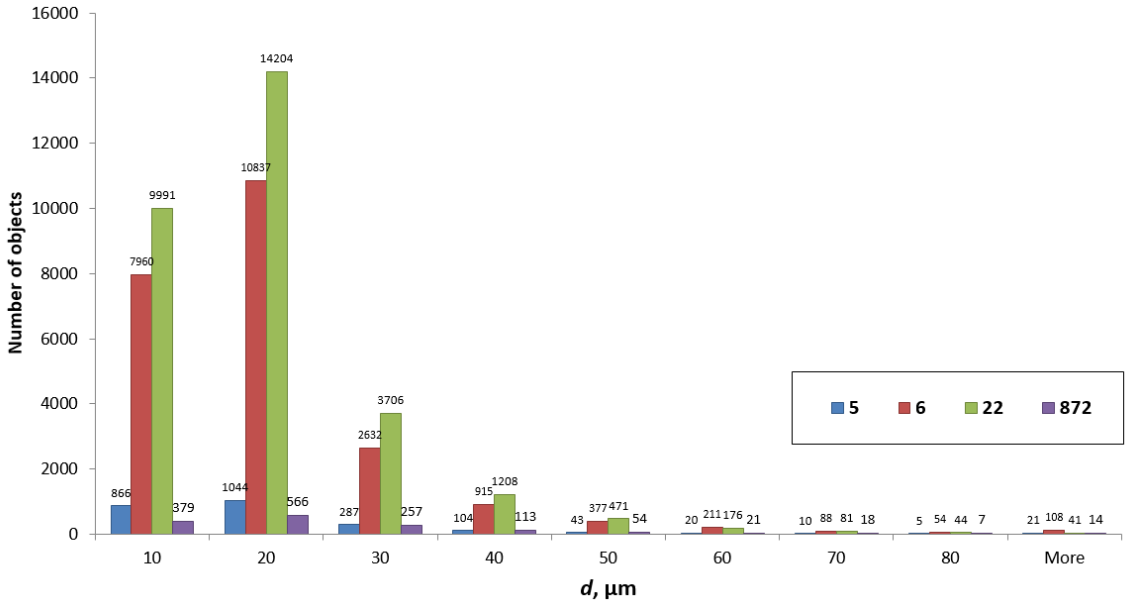


Figure 11. Distribution of pyrite diameter *d* for the all samples detected by CT results

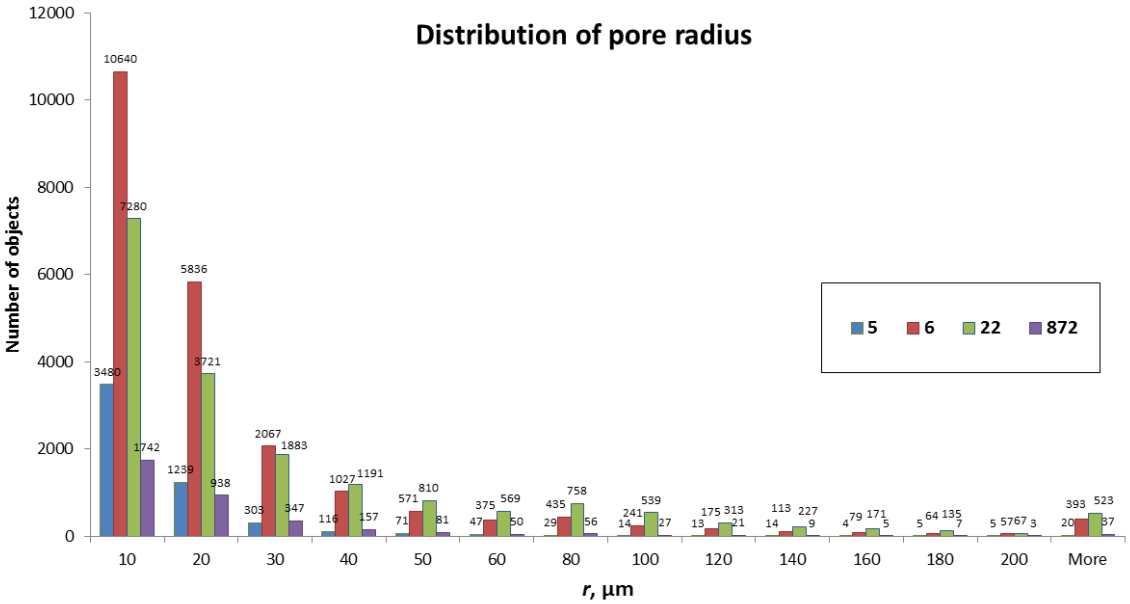


Figure 12. Distribution of pore diameter *r* for the all samples detected by CT results